Hindawi
Advances in Civil Engineering
Volume 2020, Article ID 8892686, 20 pages
https://doi.org/10.1155/2020/8892686

Research Article

Damage Identification Method of Beam Structure Based on Modal Curvature Utility Information Entropy

Chang-Sheng Xiang,[1] Ling-Yun Li ,[1] Yu Zhou ,[2] and Zi Yuan[1]

[1]*School of Civil Engineering, Lanzhou University of Technology, Lanzhou 730050, China*
[2]*College of Civil Engineering, Anhui Jianzhu University, Hefei 230601, China*

Correspondence should be addressed to Yu Zhou; yuzhou923@outlook.com

Received 16 July 2020; Revised 14 August 2020; Accepted 5 September 2020; Published 19 September 2020

Academic Editor: Songtao Lv

Generally, the damage of the structure will lead to the discontinuity of the local mode shape, which can be well reflected by the modal curvature of the structure, and the local information entropy of the beam structure will also change with the discontinuity of the mode. In this paper, based on the information entropy theory and combining the advantages of modal curvature index in damage identification of beam structure, the modal curvature utility information entropy index is proposed. The modal curvature curves of nondestructive structures were obtained by fitting the modal curvature curves of damage structures with the gapped smoothing technique to avoid dependence on the baseline data of nondestructive structures. The index comprehensively reflects the damage state of the structure by calculating mutual weight change matrix and the weight-probability coefficient. The performance of the new index was verified by the finite element simulation and model test of simply supported beam, respectively. The results show that the modal curvature utility information entropy index takes advantage of the modal curvature index which is sensitive to damage and can overcome its shortcomings effectively. The index proposed can identify the damage location and damage degree accurately and has certain noise immunity, which provides an effective damage identification indicator for beam structures.

1. Introduction

In recent years, high requirements on the integrity and performance of civil engineering structures is increasingly needed, which is reflected in the increasing complexity of civil structures, bridge structures, large stadiums, and tunnels, as well as the increasing service performance and construction scale. The safety of the beam structure is inevitably reduced due to the natural environment, material deterioration, construction defects, overload, and other factors, which may cause serious consequences. Therefore, it is of great practical significance to study the structural health monitoring (SHM) technology [1, 2].

With the use of an advanced and reliable sensor, the SHM technology has been rapid developed [3–5]. The most fashionable approaches in SHM are based on the structure vibration characteristics. These methods depend on the stiffness change on the influence of the dynamic characteristics of structure [6], which get the extensive attention of scholars because it is simple and easy. Common indicators include modal frequency [7], modal displacement [8], and the modal strain energy [9]. In view of the insufficient sensitivity of early damage identification indexes such as natural frequency and modal displacement, Pandey [10] firstly proposed a damage identification method for beam structure based on modal curvature (MC) in 1991, which has been widely applied and extended. Cao et al. [11] expounded the effectiveness of MC index and pointed out that MC is sensitive to measurement noise in waveform. In order to solve this problem, the Teager energy operator together with wavelet transform is tactically utilized to treat modal curvature; thus, a new modal curvature is put up, termed the Teager energy operator-wavelet transform (TEO-WT) modal curvature. It has been found that the combination of

continuous wavelet transform and MC can effectively filter out the modal data containing noise and reduce the impact of noise on the damage identification accuracy [2, 12]. Xu et al. [13] improved the two-dimensional modal curvature by real wavelet transform and complex wavelet transform, and wavelet 2D modal curvature is obtained. Dessi and Camerlengo [14] compared several damage identification methods based on MC and modal strain energy analysis; this analysis intends to point out comparatively the capability of locating and estimating damage of each method along with some critical issues already present with noiseless data. Zhang et al. [15] pointed out the shortcomings of MC index: (1) MC is not sensitive enough to the damage of modal nodes; (2) for the structure with multiple damages, the index of modal curvature difference cannot effectively reflect the damage degree of the structure. In order to improve the damage identification ability of MC index, some scholars obtained the analytical expression of the modal curvature change of the beam damage state by using the perturbation solution of the Euler beam motion equation, and introduced the filtering technology of the modal curvature change to establish the inverse problem of damage positioning based on the modal curvature only [16, 17]. MC index has also been popularized and applied to damage identification of plate structures based on two-dimensional mode curvature [18]. Yang et al. [19] proposed a curvature correction method incorporating bending and torsion effects into damage assessment.

Combining with the advantages of MC index to identify structural damage, entropy theory is introduced into the damage identification of beam structures. Entropy is an important concept to describe system chaos proposed by Clausius in thermodynamics. The physical meaning of entropy has different meanings in different fields, so the application of entropy presents different forms [20–23], and different forms of entropy show a promising prospect in the field of structural damage identification, such as, the transfer entropy, the approximate entropy, the fuzzy entropy and the wavelet entropy. Information entropy was first proposed by Shannon [24], which is used to characterize the disorder degree of the system signal state. Information entropy theory has been applied in the study on surrounding rock stability [25] and material damage [26]. However, relatively few studies have been conducted in the field of beam structure damage. Liu and Wu [27] introduced the theory of information entropy into the dynamic identification of damage to concrete structures, providing a new way of thinking for solving such problems as insufficient sensitivity and difficulty in nonlinear analysis in damage identification. Yang et al. [28] proposed generalized-local information entropy algorithm.

In this paper, on the basis of previous researches, based on the theory of Utility Information Entropy in Information theory, the advantages of MC in structural damage identification is make fully used and the Modal Curvature Utility Information Entropy (MCUIE) index is put forward. The effectiveness of the index is verified by using the finite element model of simply supported beam, and the practicability of the index is verified by the test of simply supported steel beam.

2. Theoretical Background

2.1. Basic Theory of Modal Curvature. In structural mechanics, the differential equation of transverse vibration of Euler beam is [29]

$$\frac{\partial^2}{\partial x^2}\left(EI(x)\frac{\partial^2 v(x,t)}{\partial x^2}\right)+m(x)\frac{\partial^2 v(x,t)}{\partial t^2}=p(x,t), \quad (1)$$

where $v(x, t)$ is the vertical vibration displacement at the beam section x at time t and $EI(x)$ is the bending stiffness of the section.

In order to better describe the vibration state of the structure, the relationship between variables is expressed in the form of function. After the structure is discretized, the vibration equation of Euler beam in the form of matrix in the elastic range can be obtained:

$$\begin{pmatrix} m(x_1) & & & 0 \\ & m(x_2) & & \\ & & \ddots & \\ 0 & & & m(x_n) \end{pmatrix}\begin{bmatrix} v_1'' \\ v_2'' \\ \vdots \\ v_n'' \end{bmatrix}+\begin{bmatrix} k_{11}[E(x_1)I(x_1)] & k_{12}[E(x_1)I(x_2)] & \cdots & k_{1n}[E(x_1)I(x_n)] \\ k_{21}[E(x_2)I(x_1)] & k_{22}[E(x_2)I(x_2)] & \cdots & k_{2n}[E(x_2)I(x_n)] \\ \vdots & \vdots & \ddots & \vdots \\ k_{n1}[E(x_n)I(x_1)] & k_{n2}[E(x_n)I(x_2)] & \cdots & k_{nn}[E(x_n)I(x_n)] \end{bmatrix}\begin{bmatrix} v_1 \\ v_2 \\ \vdots \\ v_n \end{bmatrix}=\begin{bmatrix} p(x_1,t) \\ p(x_2,t) \\ \vdots \\ p(x_n,t) \end{bmatrix}, \quad (2)$$

where, $x_1, x_2, \ldots, x_n$ is the longitudinal coordinate of node 1, 2, …, n; $m(x_n)$ is the discrete mass of node n; v_n and v_n'' are the vertical displacement and vertical acceleration of node n, respectively; $k_{ij}(E(x_i)I(x_j))$ is the stiffness coefficient component of the structure, which means the vertical force on node i when element deformation of node j occurs. $p(x_n, t)$ is the external excitation received by node n at time t.

From equation (2), it can be seen that the stiffness change at the node of the structure not only affects the displacement and curvature change of itself, but also affects the displacement and curvature of other nodes. As reflected in the practical problem, the modal curvature difference (MCD) at the structural damage will change greatly, but the undamaged part, especially near the damage location, the MCD will often be large, which leads to the misjudgment of damage identification.

The solution of equation (1) can be expressed as the superposition form of each mode:

$$v(x,t) = \sum_{j=1}^{\infty} \varphi_j(x) q_j(t), \tag{3}$$

where j is the number of mode order; $\varphi_j(x)$ and $q_j(t)$ are the j^{th} mode displacement and mode coordinates of the beam, respectively.

According to the relevant theories of beam bending deformation [15]:

$$\frac{M(x,t)}{EI(x)} = k(x,t) = \frac{\partial^2 v(x,t)}{\partial x^2} = \sum_{j=i}^{\infty} \varphi_j''(x) q_j(t), \tag{4}$$

where $M(x, t)$ is the bending moment of the beam section; $K(x, t)$ ias the curvature of beam vibration curve; and $\varphi_j''(x)$ is the j^{th} MC.

It is assumed that in the eigenvalue problem, the damage of the beam structure only affects the stiffness matrix, but not the inertia matrix [14]. According to damage mechanics, the constitutive relation of concrete damage is [16]

$$\sigma = E(1 - D)\varepsilon, \tag{5}$$

where D is the local damage factor of the structure and $E(1-D)$ is the local stiffness of the structure after damage.

According to equations (4) and (5), with the aggravation of the damage degree of the structure, the damage factor D increases while the local stiffness of the structure decreases, which finally leads to the increase of the MC at the damage.

The simply supported planar beam has negligible shear deformability. As shown in Figure 1, damage is modelled as a localized and uniform reduction of the bending stiffness distribution $K(x)$ along the dimensional coordinate x. Thus, the damaged beam of length L is considered as the union of three beam portions as shown in Figure 2, where the shortest one, with a reduced cross section with respect to the others, represents the damaged portion. For each beam portion, L_i, A_i, and K_i denote the length, cross section area, and bending stiffness, respectively. For generality, it is convenient to formulate identification methods using nondimensional coordinates ξ, η, with $\xi = x/L$ and $\eta = y/L$, and nondimensional variables. For each beam portion of nondimensional length $l_i = L_i/L$ $(i = 1, 2, 3)$, conditions at the edges are defined in terms of the boundary conditions whereas at the interfaces between the beam portions, continuity of displacement v, slope θ, bending moment M, and shear force V is imposed (all nondimensional). The generic expression of mode shapes in nondimensional form is [30, 31]

$$\begin{aligned} \varphi(x_i) = {} & A \sin a_i x_i + B \cos a_i x_i + C \sin h\, a_i x_i \\ & + D \cos h\, a_i x_i \quad i = 1, 2, 3, \end{aligned} \tag{6}$$

where A, B, C, and D are the coefficients, $a_i^4 = \omega_i^2 m_i / EI_i$ is frequency equations.

The beam boundary conditions in terms of nondimensional mode shapes are expressed as

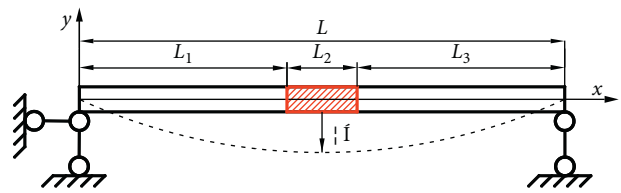

Figure 1: Simply supported beam with the damaged portion in red.

$$\begin{cases} \varphi_1(0) = 0, \\ \varphi_1''(0) = 0, \\ \text{applied in point } O_1, \end{cases} \qquad \begin{cases} \varphi_3(l_3) = 0, \\ \varphi_3''(l_3) = 0, \\ \text{applied in point } O_4. \end{cases} \tag{7}$$

Substituting the generic expression of mode shapes into the set of boundary conditions equation (7), the expressions of natural frequencies and mode shapes can be calculated [30]:

$$\omega_i^n = n^2 \pi^2 \sqrt{\frac{EI_i}{m_i L_i}} \quad (i = 1, 2, 3; n = 1, 2, \ldots, \infty), \tag{8}$$

$$\varphi_n(x_i) = A_n \sin\left(\frac{n\pi L_i}{L}\right) \quad (i = 1, 2, 3; n = 1, 2, \ldots, \infty), \tag{9}$$

where A_n is constant and depends on the initial conditions, whereas at the interfaces, the continuity of displacement, slope, bending moment, and shear force is applied [14]:

$$\begin{cases} \varphi_1(l_1) = \varphi_2(0), \\ \varphi_1'(l_1) = \varphi_2'(0), \\ \varphi_1''(l_1) = \dfrac{K_2}{K_1}\varphi_2''(0), \text{ applied in point } O_2, \\ \varphi_1'''(l_1) = \dfrac{K_2}{K_1}\varphi_2'''(0), \end{cases} \qquad \begin{cases} \varphi_2(l_2) = \varphi_3(0), \\ \varphi_2'(l_2) = \varphi_3'(0), \\ \varphi_2''(l_2) = \dfrac{K_1}{K_2}\varphi_3''(0), \text{ applied in point } O_3. \\ \varphi_2'''(l_2) = \dfrac{K_1}{K_2}\varphi_3'''(0), \end{cases} \tag{10}$$

It is worth underlying that the sudden variation of stiffness implies that curvatures lose continuity as well. The discontinuity in the bending stiffness is reflected sharply on the curvature of the mode shapes as a result of equation (10).

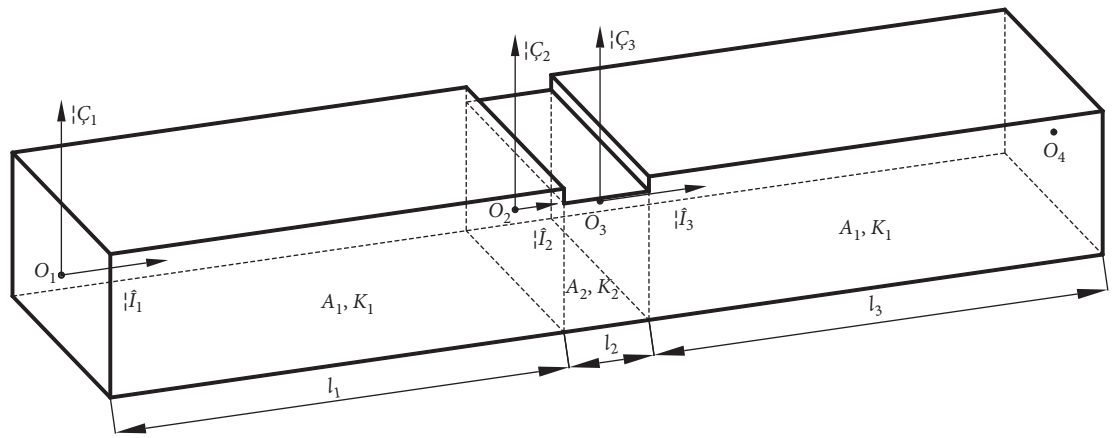

Figure 2: Geometrical nondimensional parameters of the notched beam.

The final expression for the mode-shape curvatures is quite complicate. In practical engineering, the MC of structural modes is generally approximated by the central difference method [10]:

$$\varphi_{ji}'' \approx \frac{2}{h_{i-1}+h_i}\left[\frac{\varphi_{j(i+1)}-\varphi_{ji}}{h_i}-\frac{\varphi_{ji}-\varphi_{j(i-1)}}{h_{i-1}}\right], \tag{11}$$

where φ_{ji} represents the mode displacement of the i^{th} measurement point in the j^{th} modal and h_i is the distance between the i^{th} measuring point and the $(i\text{-}1)^{\text{th}}$ measuring point.

2.2. Basic Theory of Information Entropy. Let the information space of information source X be

$$[X \cdot P]: \begin{cases} X: a_1 a_2 \cdots a_n, \\ p(X): p_1\ p_2 \cdots p_n, \end{cases} \tag{12}$$

where X: $a_1\ a_2 \ldots a_n$ is the information source symbol, $p(X)$: $p_1\ p_2\ \ldots\ p_n$ is the probability of the information source symbol, and $0 \le p_i \le 1$.

The total information contained in the information source symbol a_i $(i = 1, 2, \ldots, n)$ is called the self-information $I(a_i)$ of the information source symbol a_i, and its mathematical meaning refers to the logarithm of the reciprocal of the prior probability $p(a_i)$ of the information source symbol a_i, that is [32],

$$I(a_i) = \log\frac{1}{p(a_i)} = -\log p(a_i) \quad (i = 1, 2, \ldots, n). \tag{13}$$

The self-information function determined by equation (13) shows that the uncertainty of symbol a_i $(i = 1, 2, \ldots, n)$ emitted by information source X is a function of the prior probability $p(a_i)$ of symbol a_i, and is uniquely determined by it.

Although the self-information function $I(a_i)$ $(i = 1, 2, \ldots, n)$ can measure the information capacity well, the self-information function is random because of the uncertainty of the source symbol, which means that the source emits a certain symbol a_i $(i = 1, 2, \ldots, n)$, the amount of information provided, and it cannot represent the ability of the entire source to provide information.

In order to represent the information measure of information source X, in 1948, Shannon put forward the concept of information entropy [24]. The information entropy of the information source X is defined as statistical average of self-information $I(a_i)$ $(i = 1, 2, \ldots, n)$, which is used to represent the disorder degree and of the signal state of the system, that is [32],

$$\begin{aligned} H(X) &= p(a_1)I(a_1) + p(a_2)I(a_2) + \cdots + p(a_n)I(a_n) \\ &= -p(a_1)\log p(a_1) - p(a_2)\log p(a_2) - \cdots \\ &\quad - p(a_n)\log p(a_n) \\ &= -\sum_{i=1}^{n} p(a_i)\log p(a_i), \end{aligned} \tag{14}$$

where $H(X)$ is the information entropy of the system; P_i is the probability of the i^{th} information in the information source; and $\log P_i$ is the amount of information provided by the i^{th} information.

3. Calculation Method of MCUIE Index

3.1. Establish of the Local Probability of MC. Information entropy is a global parameter, which is capable of representing the overall characteristics of the structure. However, the damage is a local feature of the structure. When the global probability is used to describe the information of the damage point, the information of the damage point will be covered by the boundary effect. Therefore, this paper defines a set composed of n locally adjacent measurement points; $P(x)$ adopts the local probability [28] to represent the proportion of the information amount of the measurement points in the sum of the information amount of the adjacent measurement points and reflects the disorder degree of the signal state of the measurement points:

$$p_i = \frac{\varphi_i''}{\sum_{i=0}^{n} \varphi_i''}, \tag{15}$$

where φ_i'' is the MC of the i^{th} node and n represents the number of nodes.

When calculating the local probability P_i of the i^{th} node, the front and rear nodes adjacent to the i node are taken as auxiliary calculation points, the calculation points, and auxiliary points form a sliding window to calculate the local probability of each point in turn, as shown in Figure 3.

For the calculation of the local probability of second-order MC, the negative and positive offset will occur near the zero point of the MC, so that the denominator of equation (15) will be reduced to close to zero, and the value of P_i will jump greatly, i.e., "false peak" will appear, affecting the accuracy of structural damage identification. Therefore, it is necessary to process the second-order MC data to eliminate the influence of "false peak". The specific operation step is as follows:

(1) Take the absolute value of the data under a certain damage case and normalize it.

(2) Return the normalized data to the positive and negative states before the absolute value is taken, so as to ensure the change trend of the data remains unchanged.

(3) Add value "1" to the data processed in the previous step to eliminate the offset between the positive and negative data.

(4) Calculate the local probability of the data processed above.

Taking the local probability of MC of damage cases (5(40%), 20(20%), 30(10%), 50(60%); (5(40%) indicates that 40% damage occurred in element 5) as an example, the effect of data processing is illustrated, as shown in Figure 4.

From Figure 4(a), it can be seen that the local probability of the untreated data will show a large peak at the mode node (element 30), which covers the real damage situation. Figure 4(b) shows that the variation trend of the local probability curve of the processed data conforms to the actual situation of the damage.

3.2. Gapped Smoothing Technique. Most of the structural damage identification indexes require the modal data before and after the structural damage as input parameters, but the modal parameters of the undamaged structure state are often difficult to obtain. The basic idea of gapped smoothing technique (GST) is that modal characterization such as mode shape and curvature mode shape of a healthy structure has a smooth shape, which can be approximated by a polynomial in two or three variables. For damaged structures, the modal characterization is no longer smooth in the whole space and irregular mutation is induced where local damages exist. With the modal curvature information of the undamaged structure being unknown, the modal curvature value of the damage point of the structure can be removed, and the smooth curve can be fitted by using the gapped smoothing technique to approximate replace the modal curvature curve of the undamaged structure. This technique was originally developed by Ratcliffe [33]. A similar method is the Chebyshev polynomial fitting technique [34]. The curve fitting function is a quartic polynomial described by equation (16), where $F(x)$ is the mode shape curvature of the beam.

$$F(x) = c_4 x^4 + c_3 x^3 + c_2 x^2 + c_1 x + c_0. \tag{16}$$

For example, the modal curvature before and after the single point damage of simply supported beam structure is shown in Figure 5. It can be seen that the MC curve at the damage location has a significant mutation. The MC curve equation of the structure in the undamaged state and the approximate modal curvature curve equation of the structure in the undamaged state fitted by gapped smoothing technique are as follows:

$$\begin{aligned} F_1(x) = {} & (-5.642e-8)x^4 + (6.996e-6)x^3 \\ & - (5.009e-5)x^2 - 0.01034x + 0.0102, \end{aligned} \tag{17}$$

$$\begin{aligned} F_2(x) = {} & (-5.601e-8)x^4 + (6.945e-6)x^3 \\ & + (4.984e-5)x^2 - 0.01026x + 0.0101. \end{aligned} \tag{18}$$

The MC curve fitted by the undamaged beam and GST as indicated by equations (17) and (18) is shown in Figure 6. It can be seen that the two curves almost coincide. By using the corrcoef (X, Y) function in MATLAB, the Pearson correlation coefficient of the two curves can be calculated to be equal to 1, i.e., the two curves are completely correlated, indicating that it is feasible to replace the modal curvature curve in the undamaged state of the structure with the MC curve obtained by GST fitting.

3.3. Calculation of MCUIE Index. Let the utility space of information source X be

$$[X \cdot W]: \begin{cases} X: a_1 a_2 \cdots a_n, \\ W(X): w_{11} w_{ij} \cdots w_{nn}, \end{cases} \tag{19}$$

where $w_{ij} \geq 0 \, (i = 1, 2, \ldots, n; j = 1, 2, \ldots, n)$ is the utility weight coefficient and represents the relative importance of the source symbol $a_i \, (i = 1, 2, \ldots, n)$ to the source symbol $a_j \, (j = 1, 2, \ldots, n)$.

In this paper, we take the value of pairwise division of the elements in the source symbol as its relative importance; then a mutual weight matrix $H(w)$ of order $n \times n$ can be obtained. In theory, when the structure is damaged, the MC of the damaged node will be changed in the corresponding rows and columns in the mutual weight matrix, while the corresponding rows and columns of the undamaged node will remain unchanged, which indicates that when the damage occurs, the disorder degree of the relative

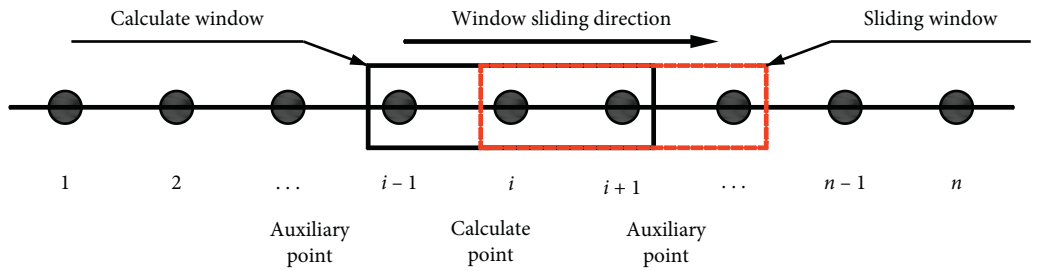

Figure 3: Description of local probability calculation.

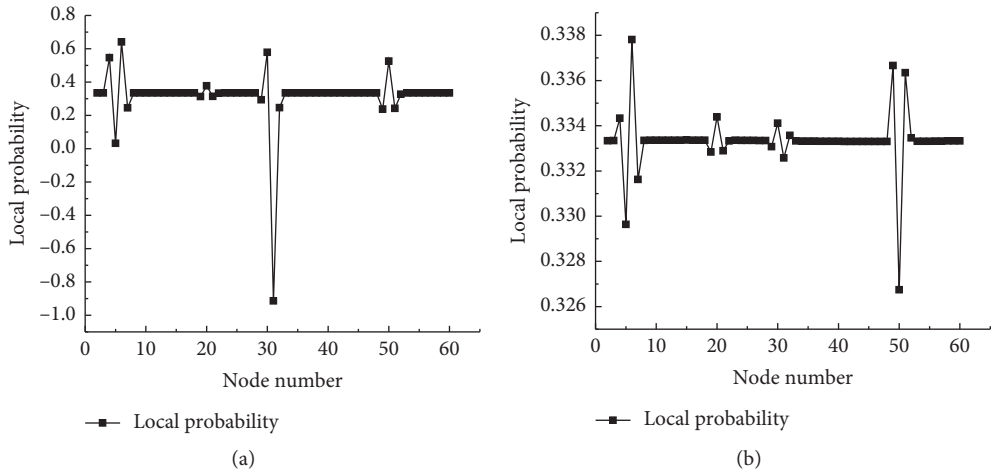

Figure 4: Local probability of modal curvature. (a) Original local probability. (b) Modified local probability.

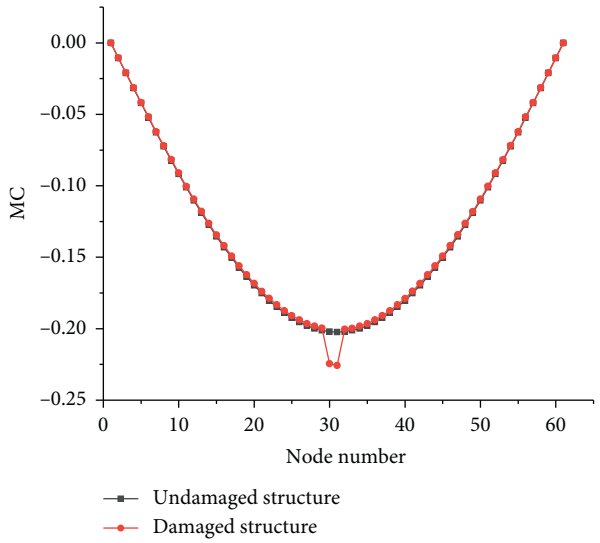

Figure 5: MC curves of structure before and after.

information of the damage node increases. This makes use of the subjective utility value and objective probability information of node modal information.

The expression of mutual weight matrix $H(w)$ is

$$H(w) = \begin{array}{c} \\ a_1 \\ a_2 \\ \vdots \\ a_n \end{array} \begin{array}{c} \begin{array}{cccc} a_1 & a_2 & \cdots & a_n \end{array} \\ \begin{bmatrix} a_{11} & a_{12} & \cdots & a_{1n} \\ a_{21} & a_{22} & \cdots & a_{2n} \\ \vdots & \vdots & \ddots & \vdots \\ a_{n1} & a_{n2} & \cdots & a_{nn} \end{bmatrix} \end{array} \tag{20}$$

where $a_{ij} = (a_i/a_j)(i = 1, 2, \ldots, n;\ j = 1, 2, \ldots, n)$, n is the number of nodes.

Suppose the mutual weight change matrix Δ before and after structural damage is

$$\begin{aligned} \Delta &= H(w)_u - H(w)_d \\ &= \begin{bmatrix} \Delta_{11} & \Delta_{12} & \cdots & \Delta_{1n} \\ \Delta_{21} & \Delta_{22} & \cdots & \Delta_{2n} \\ \vdots & \vdots & \ddots & \vdots \\ \Delta_{n1} & \Delta_{n2} & \cdots & \Delta_{nn} \end{bmatrix}, \end{aligned} \tag{21}$$

where $H(w)_u$ and $H(w)_d$ are the mutual weight matrix before and after structural damage, respectively; and the

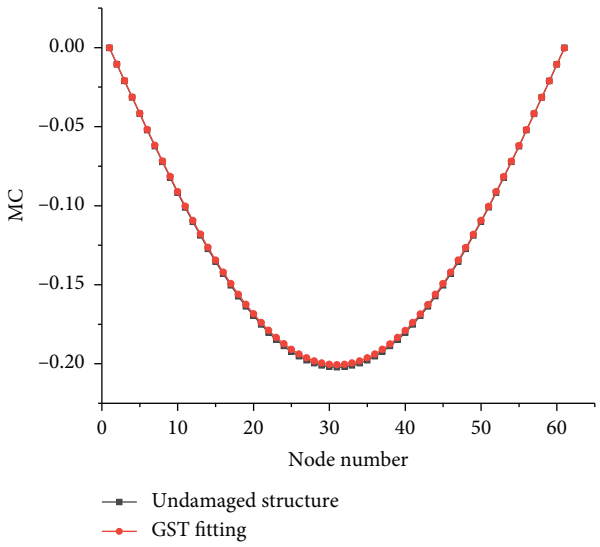

Figure 6: Gapped smoothing technique fitting.

subscripts "u" and "d" represent the undamaged and damaged states of the structure, respectively.

The MC of the damaged nodes also mutates in the corresponding rows and columns in the mutual weight change matrix, and the degree of mutation is proportional to the mutation value of the MC. When the modal curvature changes at the damage before and after the damage, the MC trend curve of the whole beam will shrink slightly, which indicates that the damage elements affect the stability of the surrounding undamaged elements to some degree, as shown in Figure 7.

To facilitate the explanation of the new index, two functions are defined: $\mathrm{sum}(\Delta)$ represents the sum of the elements of the mutual weight change matrix Δ by rows and $\mathrm{mul}(\Delta \cdot p)$ is expressed as the product of the sum of the utility weight coefficients of the source symbol $a_i \quad (i = 1, 2, \ldots, n)$ and the local probability $p_i \quad (i = 1, 2, \ldots, n)$ of the source symbol, i.e., the weighted-probability coefficient.

The weighted sum of $\mathrm{mul}(\Delta \cdot p)$ and the self-information $I(a_i) = -\log p_i \quad (i = 1, 2, \ldots, n)$ of the source symbol is defined as the modal curvature utility information entropy of the system

$$\begin{aligned}\mathrm{MCUIE} &= H_W(\mathrm{mul}_1, \mathrm{mul}_2, \ldots, \mathrm{mul}_n; I_1, I_2, \ldots, I_n) \\ &= -\mathrm{mul}_1 \log p_1 - \mathrm{mul}_2 \log p_2 - \cdots - \mathrm{mul}_n \log p_n \\ &= -\{\mathrm{mul}_1 \log p_1 + \mathrm{mul}_2 \log p_2 + \cdots + \mathrm{mul}_n \log p_n\} \\ &= -\sum_{i=1}^{n} \mathrm{mul}_i \log p_i,\end{aligned} \tag{22}$$

that is,

$$\mathrm{MCUIE} = -\sum_{i=1}^{n} mul_i \log p_i. \tag{23}$$

To some degree, the weight-probability coefficient $\mathrm{mul}_i \, (i = 1, 2, \ldots, n)$ reflects the influence of the change of the structure's overall stress characteristics on the deformation of the structure points. The self-information $I(a_i) = -\log p_i \, (i = 1, 2, \ldots, n)$ of the source symbol reflects the amount of information that the changes of structural nodes can provide to identify the overall deformation of the structure.

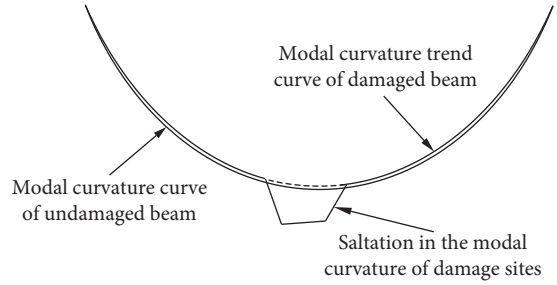

Figure 7: Change of modal curvature cure.

The specific steps of MCUIE index calculation are as follows in Figure 8:

3.4. Damage Degree Identification Method Based on MCUIE Index. The MC of element $D(x)$ without damage is ϕ_E; theoretically, the MC of element $D(x)$ after damage should be mutation from ϕ_{NA} to ϕ_{NB}, and the actual result ϕ_{NE} is the average value of ϕ_{NA} and ϕ_{NB}, as shown in Figure 9 [15].

In this paper, by considering the relationship between element damage and "node damage," the MATLAB polynomial fitting method is adopted to obtain the relationship curve between MCUIE peak at the damaged node and element damage degree, so as to judge the damage degree of the structure.

The sum of squared errors (SSE) is used as the index to evaluate the effect of curve fitting:

$$\mathrm{SSE} = \sum_{i=1}^{r} \sum_{j=1}^{ni} \left(x_{ij} - \overline{x}_i\right)^2, \tag{24}$$

where r, ni, x_{ij}, and $\overline{x}_i$ are the total number of observed data, the number of observed data, the fitting data of the j^{th} data in the i^{th} population, and the average value of the i^{th} observation data.

The closer *SSE* is to 0, the closer the linear correlation between the fitting data and the fitting function is, and the better the fitting effect is.

4. Finite Element Numerical Analysis of MCUIE Index

4.1. Establishment of Simply Supported Beam Model. The simply supported beam model was established in MIDAS/Civil, and the beam structure was divided into 60 equally spaced elements, as shown in Figure 10. The span of simply supported beam is $L = 6$ m with a section size 0.6 m × 0.4 m. C40 concrete is applied with a elastic modulus $E = 3.25 \times 107\ \mathrm{kN/m^2}$ and Poisson ratio $\mu = 0.2$. The bulk density is $c = 25\ \mathrm{kN/m^3}$ and mass density is $2.549\ \mathrm{kN/m^3/g}$.

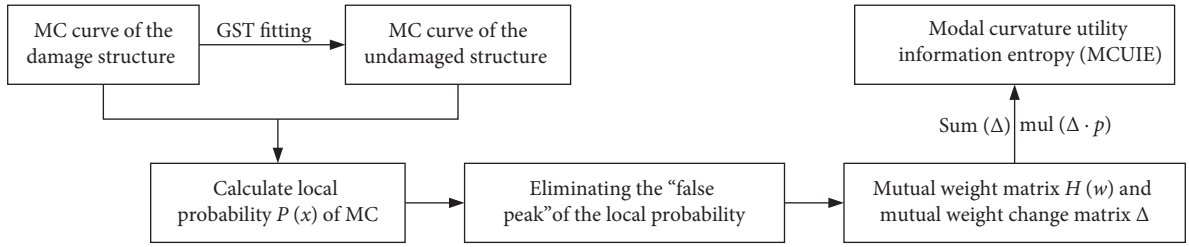

Figure 8: Calculation process of MCUIE index.

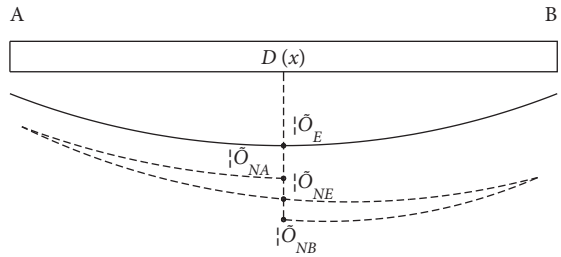

Figure 9: Relationship between element damage and node damage.

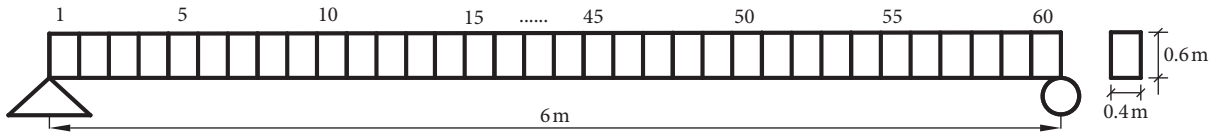

Figure 10: Simply supported beam Finite element model.

Table 1: Damage case studies in simply supported beam.

Damage case	Damage element	Damage degree (%)
1	5 20 30 50	5 60 30 20
2	5 20 30 50	20 40 60 10
3	5 20 30 50	40 20 10 60
4	1 20 35	10 20 30 40 50
5	30	5 10 20 30 40 60

Here the damage of the structure is simulated by the reduction of the element elastic modulus.

4.2. Setting of Damage Cases of Simply Supported Beam Model. The damage cases of single point, multiple points with the same damage degree, and different damage degrees were set to verify the effectiveness of MCUIE index, and the damage cases of simply supported beam are shown in Table 1.

The calculation results of the first-two order frequencies and periods of the simply supported beam model are shown in Table 2.

By comparison, with the aggravation of the beam structure damage (the degradation of the element stiffness), the natural frequency of the beam structure gradually decreases and the period gradually increases.

4.3. Damage Identification Results Analysis of MCUIE. The first-two modal damage identification results are given in this section. Figures 11–13 show the damage identification comparison result of the first-two orders of MCUIE index and MCD index [18] in the above damage cases. When the structure is damaged, the MCUIE curve and MCD curve will undergo saltation at the corresponding damage location.

The identification results of damage cases 1–3 under the MCD are shown in Figures 11(a) and 11(b); the value of MCD index shows an obvious peak at the set damage position, so the damage position of the structure can be located. However, there are anomalies near the supports at both ends of the beam structure, and in the identification results of the second-order modes, the value of MCD index at the damage of the modal nodes is 0. Because the modal curvature at the second-order modal nodes is positive and negative offset, which negatively influences the identification of the relative damage degree of the structure.

In contrast, the MCUIE index is modified by local probability to measure the structural damage from the

Table 2: Modal information of simply supported beam.

Damage case	First-order frequency (rad/sec)	First-order period (sec)	Second-order frequency (rad/sec)	Second-order period (sec)
Undamaged	167.568	0.0375	648.129	0.00969
Single damage	166.412	0.0377	647.713	0.00971
Multiple damage	165.611	0.0379	643.143	0.00977

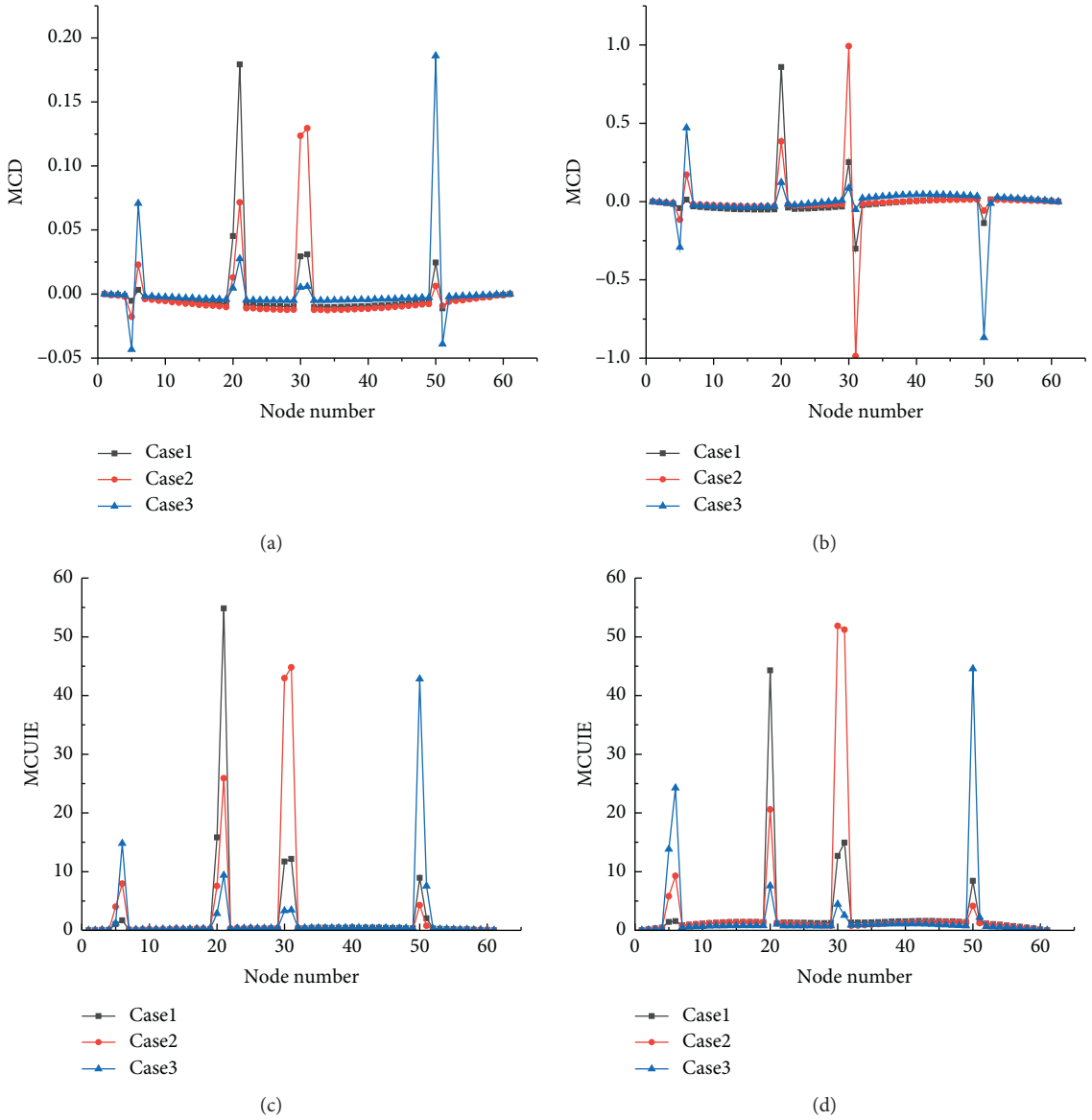

Figure 11: Damage identification results of MCD and MCIUE index of case studies 1–3. (a) First-order MCD. (b) Second-order MCD. (c) First-order MCUIE. (d) Second-order MCUIE.

perspective of probability, it can also accurately locate the damage position in Figures 11(c) and 11(d), and the identification results of the first-two modes can truly reflect the damage situation of the structure without any abnormal. With the increase of the damage degree, the MCUIE index value at the damage location also increases and increases synchronously in accordance with the proportion of the damage degree.

The identification results of case 4 are shown in Figure 12. When the same damage degree occurs at different positions of the structure, the peak value of MCUIE index of each damage position is very close, while the value of MCD index identification results varies greatly.

By comparing Figure 13, it can be seen that in the case of single point damage, the damage identification result of MCUIE index is also better than MCD index. In MCUIE

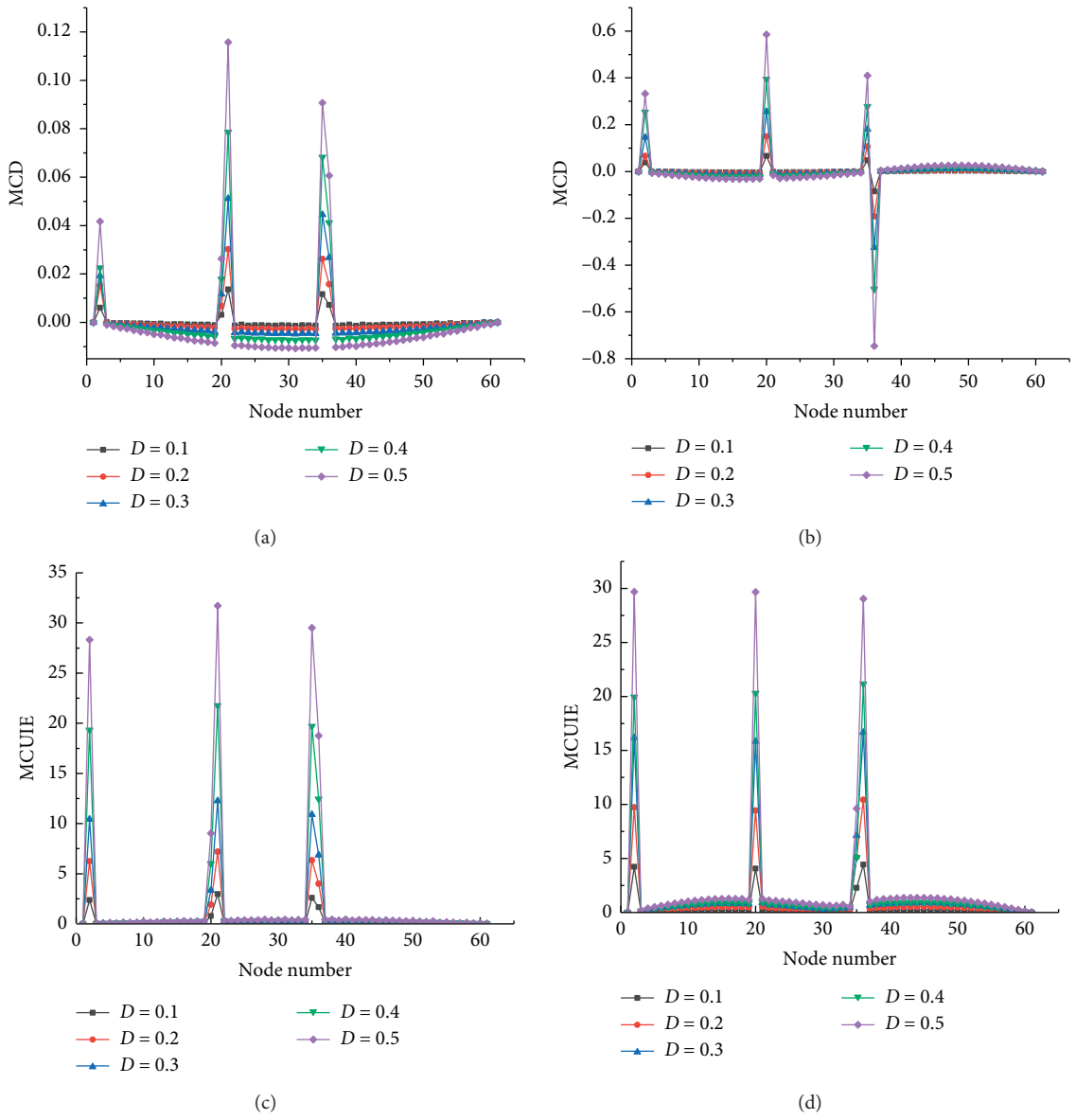

Figure 12: Damage identification results of MCD and MCUIE index of case studies 4. (a) First-order MCD. (b) Second-order MCD. (c) First-order MCUIE. (d) Second-order MCUIE.

index identification, the index has a promising sensitivity to damage when a single point of structure is damaged to a different degree, and with the aggravation of damage, the MCUIE value at the damage position increases in proportion to the damage degree of the structure, which can qualitatively reflect the damage degree of the structure.

4.4. Calculation of Structural Damage Degree. Regarding the calculation of damage degree, MATLAB is used in this paper to obtain the relationship curve between the peak value of MCUIE at damage node and damage degree by polynomial fitting method to judge the damage degree of the structure.

When a single damage with different degrees occurs in the structure (Case 5), the peak value of MCUIE at damage node is shown in Table 3 (first-order value). The relation curve of MCUIE peak value and damage degree is fitted, and the polynomial degree is 3; the damage degree function equation of structure when damage occurs in element 30 is obtained:

$$y = 151.2x^3 - 32.68x^2 + 38.88x - 0.2222, \text{SSE} = 4.5853e - 30. \quad (25)$$

The validity of equation (25) was verified by taking the index peak values of 15% and 55% as damage degree in Case 5, respectively. The results are shown in Table 4.

It can be seen from Table 4 that, for the functional equation of damage degree of a single point, the fitting error of both small damage and large damage is less than 10%,

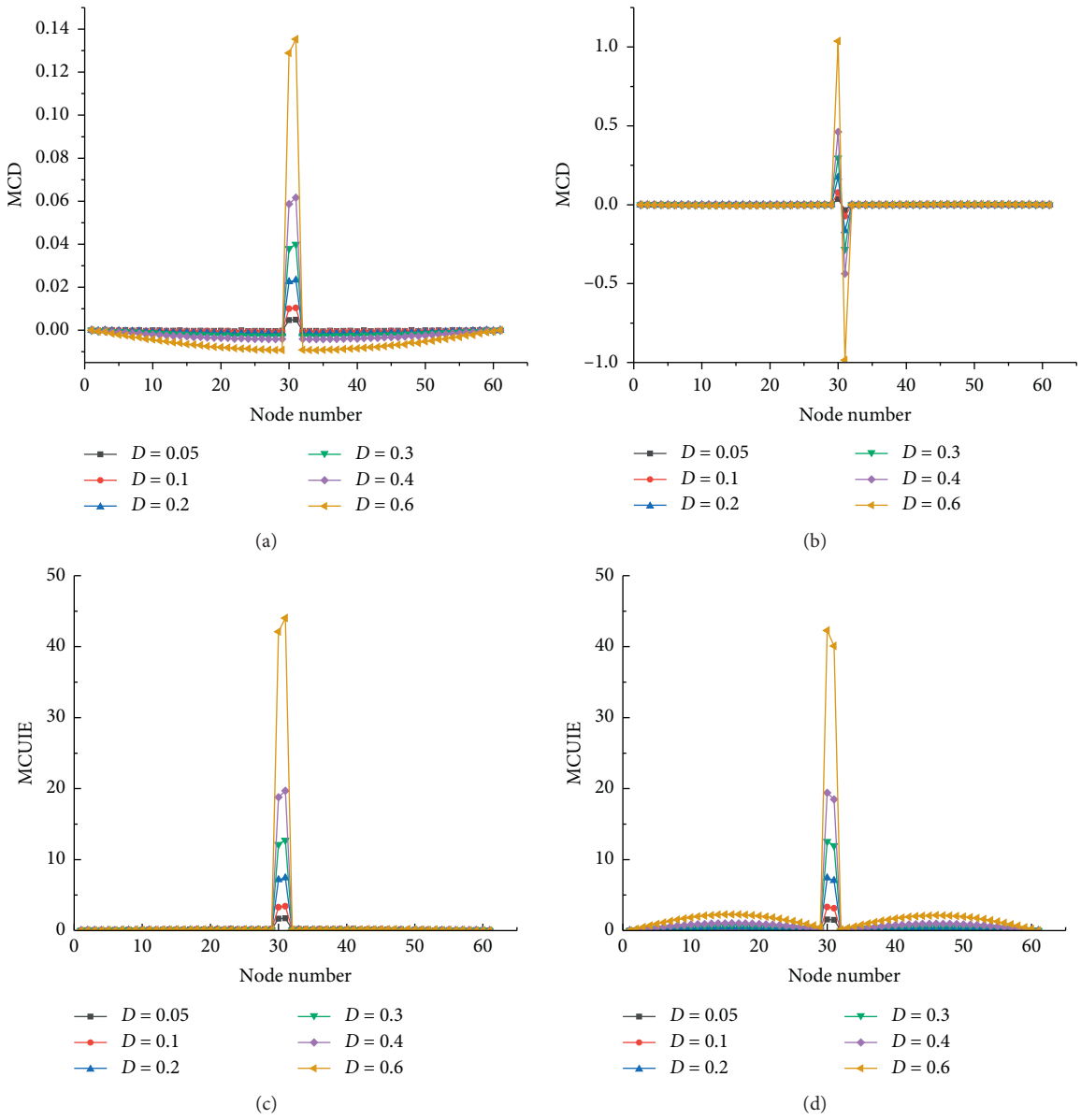

Figure 13: Damage identification results of MDC and MCUIE index of case studies 5. (a) First-order MCD. (b) Second-order MCD. (c) First-order MCUIE. (d) Second-order MCUIE.

Table 3: MCUIE value of Single damage with different damage degrees.

Damage element	Damage degree (%)	MCUIE value
30	5	1.6591
	10	3.4902
	20	7.4562
	30	12.5832
	40	19.7782
	60	44.0021

indicating that equation (25) of damage degree fitting is effective and feasible.

Structural damage relationship fitting curve is shown in Figure 14; as can be seen from the graph, with the increase of damage degree, MCUIE value of damage node increases gradually, when damage degree is greater than 40%, the damage growth curve is nonlinear. Considering the cumulative effect of structure damage, the relationship of damage can be qualitatively verified the rationality of the fitted curve growth trend.

Table 4: Validation of single damage degree function equation.

Damage element	Damage degree (%)	Calculated value	Fitted value	Identification error
30	15	5.982	5.385	9.9
	55	37.855	36.432	3.8

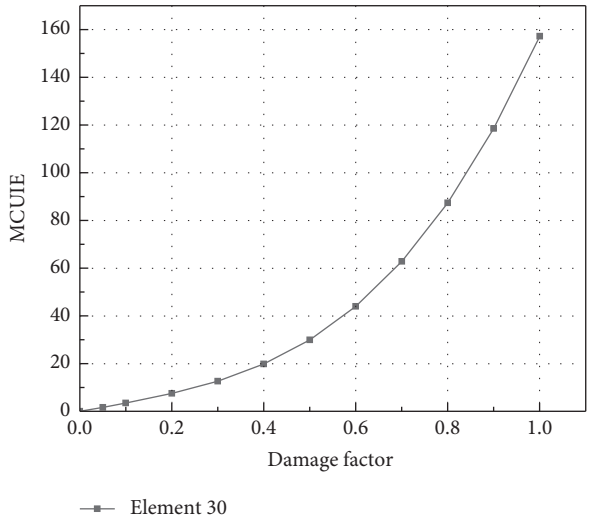

Figure 14: Damage degree fitting curve of single damage.

Table 5: MCUIE value of multidamage with different damage degrees.

Damage element	MCUIE value of element with different damage degrees				
Damage degree (%)	10	20	30	40	50
1	2.3745	6.0944	11.533	19.3256	28.3274
20	2.9621	7.1848	13.311	21.7613	31.7177
35	2.5933	6.3385	11.727	19.7066	29.5062

Table 6: Validation of multidamage degree function equation.

Damage element	Damage degree (%)	Calculated value	Fitted value	Identification error (%)
1	15	4.484	3.918	12.6
20	45	27.514	26.501	3.75

The damage degree of structure with multiple points and different damage degrees is calculated by taking case 4 as an example. MCUIE peak value of the damaged node is shown in Table 5 (first-order value). The relationship curve between the peak value of MCUIE at damaged node and the damage degree can be obtained by fitting the data in Table 5:

$$y_1 = -42.45x^3 + 130.5x^2 - 0.243x + 1.162, \mathrm{SSE}_1 = 0.0341, \quad (26)$$

$$y_2 = -33.11x^3 + 128.3x^2 + 5.166x + 1.213, \mathrm{SSE}_2 = 0.0219, \quad (27)$$

$$y_3 = 14.74x^3 + 91.73x^2 + 7.677x + 0.918, \mathrm{SSE}_3 = 0.0422. \quad (28)$$

The damage degree fitting equations (26) and (27) of multipoint damage case were verified by taking the index peak values when the damage degrees of element 1 and 20 in case 4 were 15% and 45%, respectively. The results shown in Table 6.

The damage degree fitting curve is shown in Figure 15, comparing the damage degree fitting curves of element 1, 20, and 35, it can be seen that the damage degree fitting curves vary at different positions. Under the same damage degree, the fitting curve of element 35 near the span is above element 1 near the support, indicating that under the same damage degree, the closer the damage node is to the span, the larger the MCUIE is. Besides, with the aggravation of damage, the difference between the two curves becomes larger. Under the same damage degree, the damage degree fitting curve of element 20 is above elements 1 and 35, indicating that the damage of element on both sides of the damage location

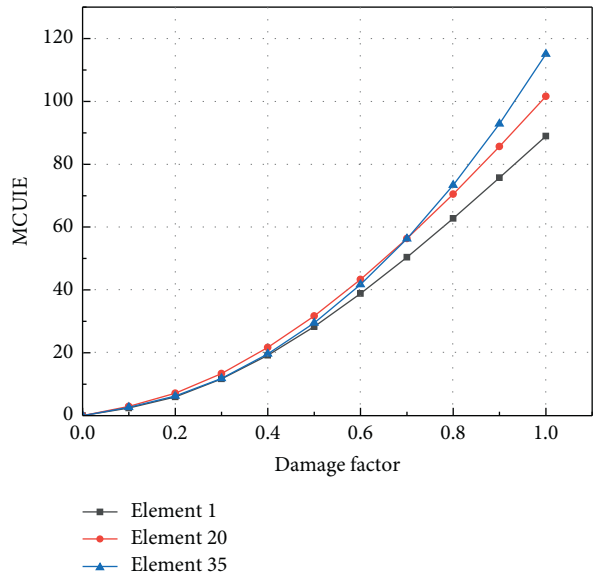

Figure 15: Damage degree fitting curve of multidamage.

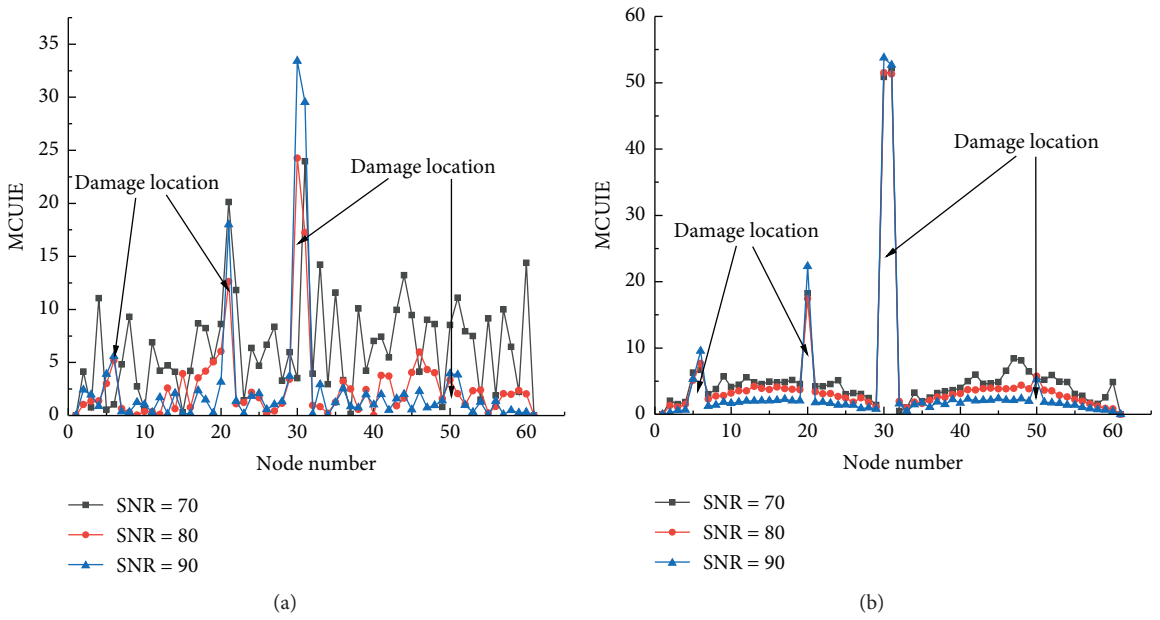

Figure 16: Antinoise verification of MCUIE index. (a) Antinoise verification of first-order. (b) Antinoise verification of second-order.

plays an aggravating role. When the damage degree reaches a certain threshold, the damage degree fitting curve of element 20 is between elements 1 and 35.

4.5. MCUIE Index Antinoise Performance Verification. To verify the antinoise performance of MCUIE index, Gaussian white noise with signal to noise ratio (SNR) of 70 dB, 80 dB, and 90 dB was added to the mode shape to simulate the noise interference.

$$\mathrm{SNR} = 10\log_{10}\left(\frac{P_s}{P_n}\right), \tag{29}$$

where P_s is the effective power of the original signal, P_n is the effective power of the noise signal, and the length of the original signal and the noise signal are consistent.

The damage identification results after adding Gaussian white noise to the mode shape of Case 2 are shown in Figure 16.

It can be seen from Figure 16 that MCUIE index has promising antinoise performance, but when the SNR of first-order index is equal 70 dB, the damage identification effect with a small damage degree is unsatisfactory. By comparing the results of antinoise analysis of the first-two order MCUIE indexes, it can be seen that the second-order indexes have

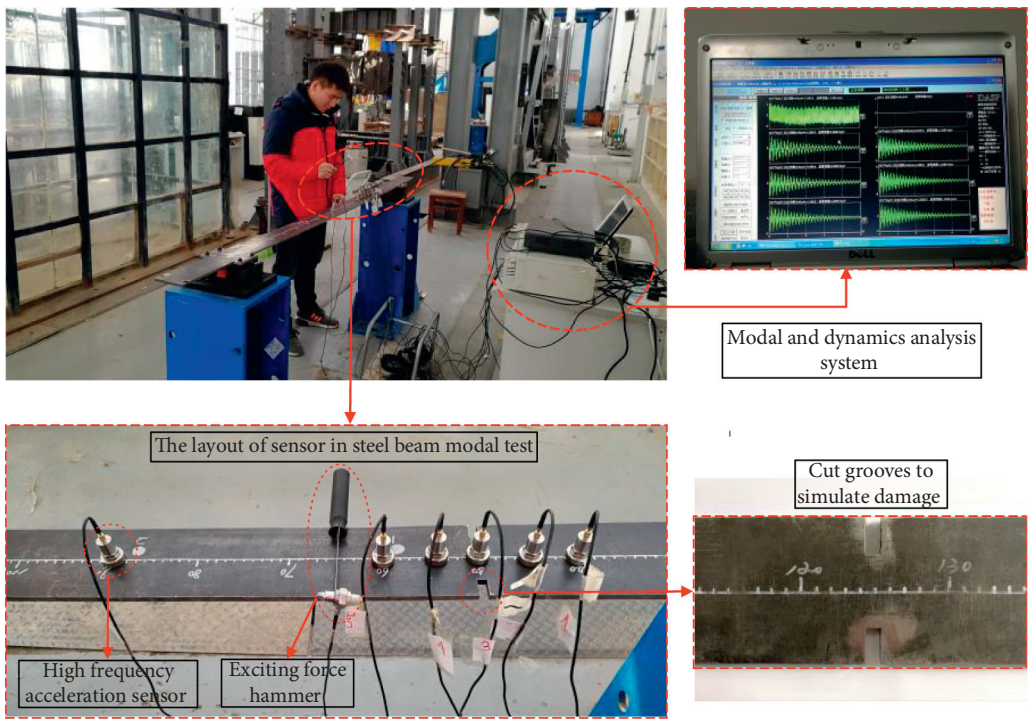

Figure 17: Test site.

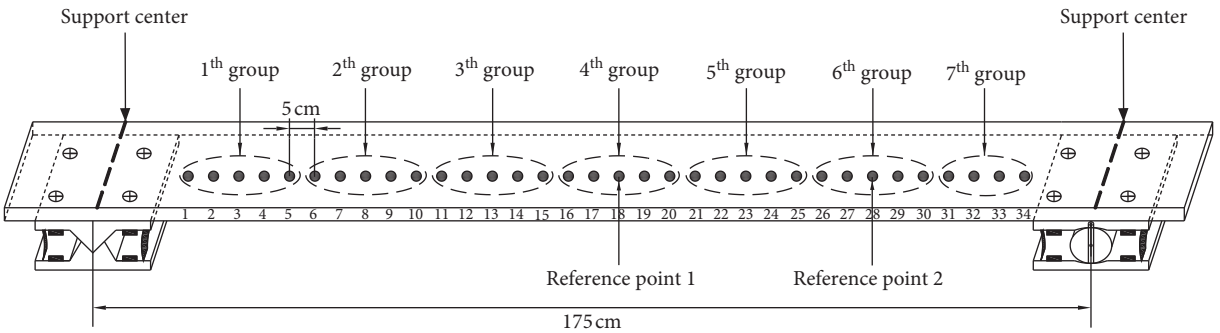

Figure 18: Monitoring point arrangement.

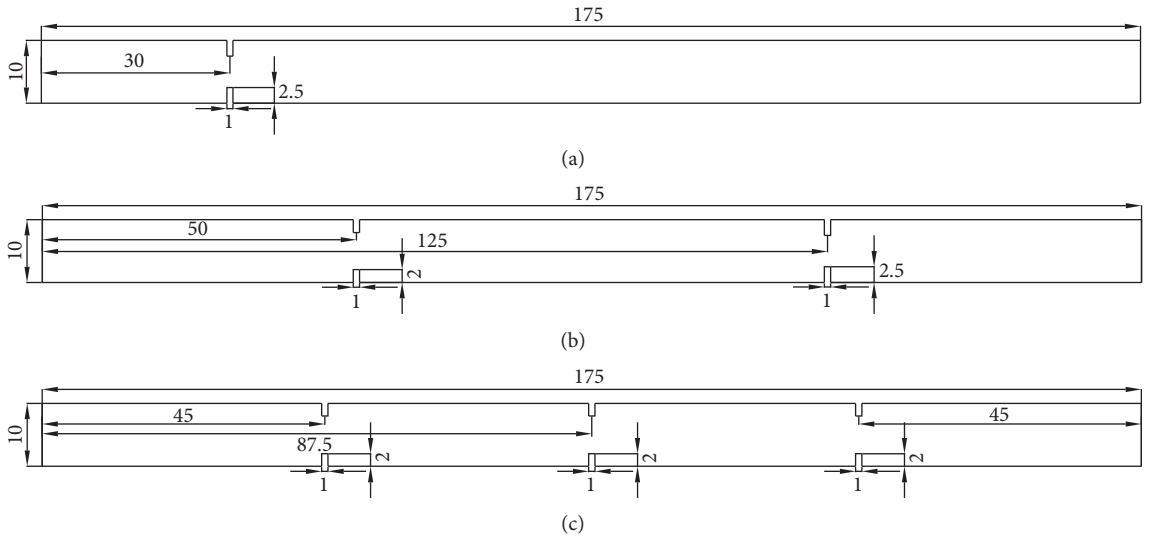

Figure 19: Steel beam damage setting (unit: cm). (a) Single damage. (b) Two damage. (c) Three damage.

Table 7: Test simulation damage cases.

Damage cases	Cutting cases (incision width of 1 cm)	Damage degree (%)
6	Incision depth was 2.5 cm at 30 cm	50
7	Incision depth was 2.0 cm and 2.5 cm at 50 cm and 125 cm	40, 50
8	Incision depth was 2.0 cm at 45 cm, 87.5 cm and 130 cm	40

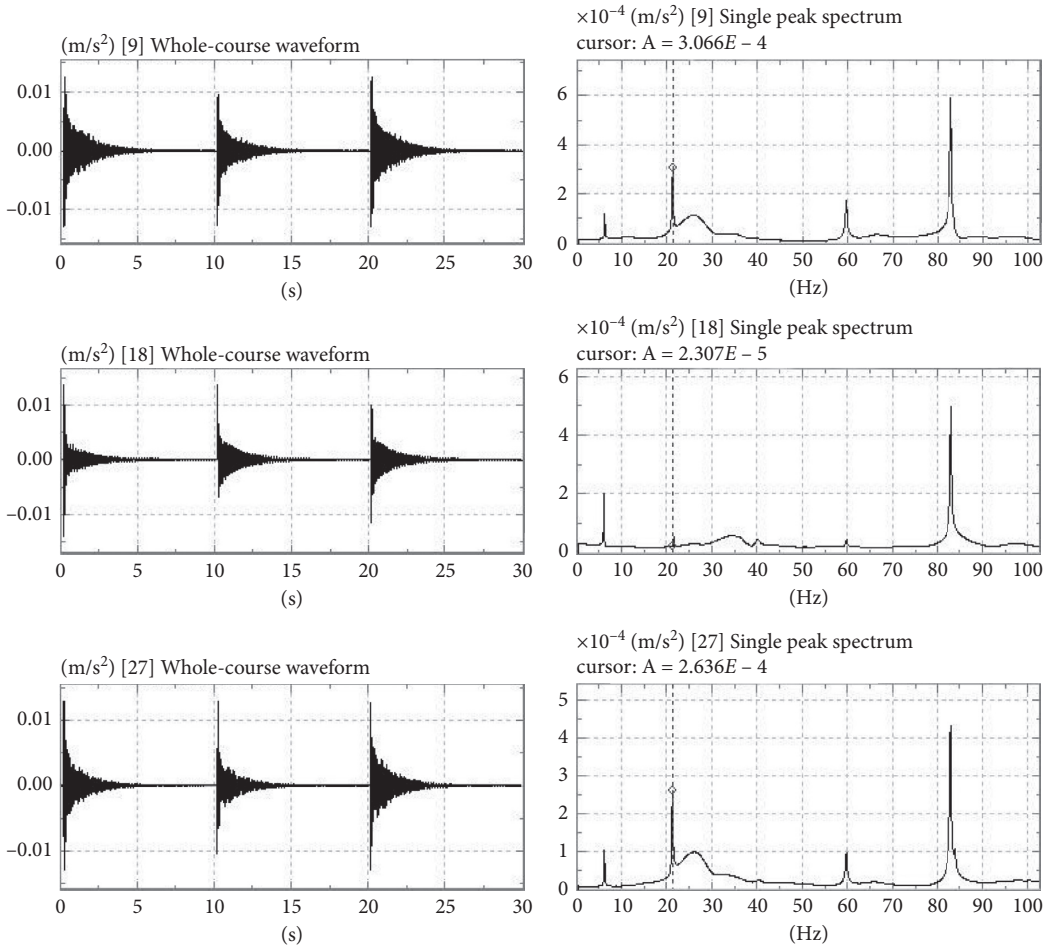

Figure 20: Spectrum curve of undamaged beam.

better antinoise performance, and the minor damage can be effectively identified, and the variation trend of MCUIE peak at the damage node is basically consistent with the variation trend of damage degree.

5. Test Verification of Simply Supported Beam

5.1. Design of Experimental Model. The model of simply supported steel beam with uniform section is taken as the research object to verify the effectiveness of the MCUIE index. The cross section size of the model is 100 mm × 8 mm, the model span is 175 cm, and 35 elements, 36 nodes are divided. The elastic modulus of the experimental model material $E = 2.0795 \times 108\,\text{kN/m}^2$, the bulk density $c = 76.98\,\text{kN/m}^3$, and Poisson ratio $\mu = 0.3$. The two ends of the steel beam are fixed on the prefabricated hinge support and rolling fabrication by high-strength bolts, and the acceleration sensor is installed at the element node to obtain the modal data of the structure. The single point hammer excitation force multipoint acceleration collected for simply supported steel beam, as shown in Figure 17.

With six acceleration sensors available, in order to obtain the first-two modes information of the structure more accurately, the reference point is set at the "reference point 1" in the midspan position to obtain the first-order mode information of the structure, and the "reference point 2" along the 3/4 of the span direction to obtain the second-order mode information of the structure, as shown in Figure 18.

5.2. Structural Damage Simulation and Damage Cases Setting. The section of the beam is symmetrically cut to simulate the damage; the damage form of the simulated steel beam is shown in Figure 19.

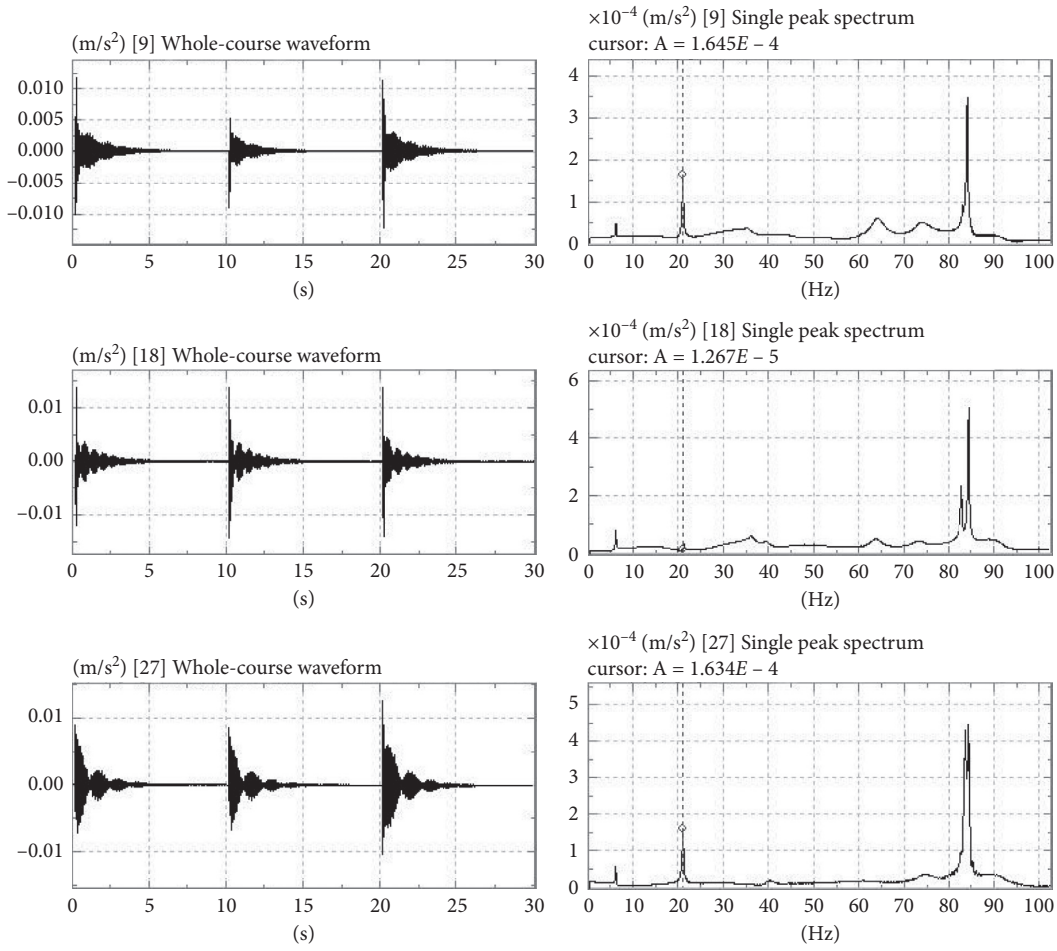

Figure 21: Spectrum curve of case 6.

For any small segment of a simply supported beam of equal section, assuming that the bending moment M is the same everywhere in the section, the maximum total bending deformation of this segment is the sum of the maximum bending deformation of each segment, as shown in the following equation:

$$\frac{L}{EI} = \frac{L_1}{EI_1} + \frac{L_2}{EI_2}, \tag{30}$$

where EI is the equivalent stiffness of any small segment, EI_1 and EI_2 are stiffness of L_1 and L_2 segments, respectively. According to equation (30), the damage degree of each damage case can be calculated, and then the damage cases of the simulated steel beam can be obtained, as shown in Table 7.

5.3. Analysis of MCUIE Method Test Verification. The random subspace method is used to calculate the modal frequency and mode data of the structure, the acceleration time-history curve is processed by fast Fourier transform, and the corresponding spectrum curve is obtained. The spectrum curve of the undamaged and damaged structure is shown in Figures 20–23.

According to equation (12), the first-two MC of the structure under each damage case can be obtained according to the modal information obtained from the test, as shown in Figure 24 (take the second-order identification result as an example). According to the calculation results of MC of damaged structures, there is an obvious abrupt peak point at the damage location, which can well show the damage location of structures, but the defects of MC index are prominent as well. For example, the linear relationship between the MC value and the damage degree of the damage point is poor, and it is not sensitive to the damage at the mode shape node.

The measured MC of the structure is abnormal near the support, which may be caused by the disturbance of the support link, the field noise, the defect of the test member, and the error of the test instrument, but it has little effect on the effectiveness of the proposed method.

According to the calculation method above, the MCUIE relation curve under each damage case is obtained by processing the measured modal data of the

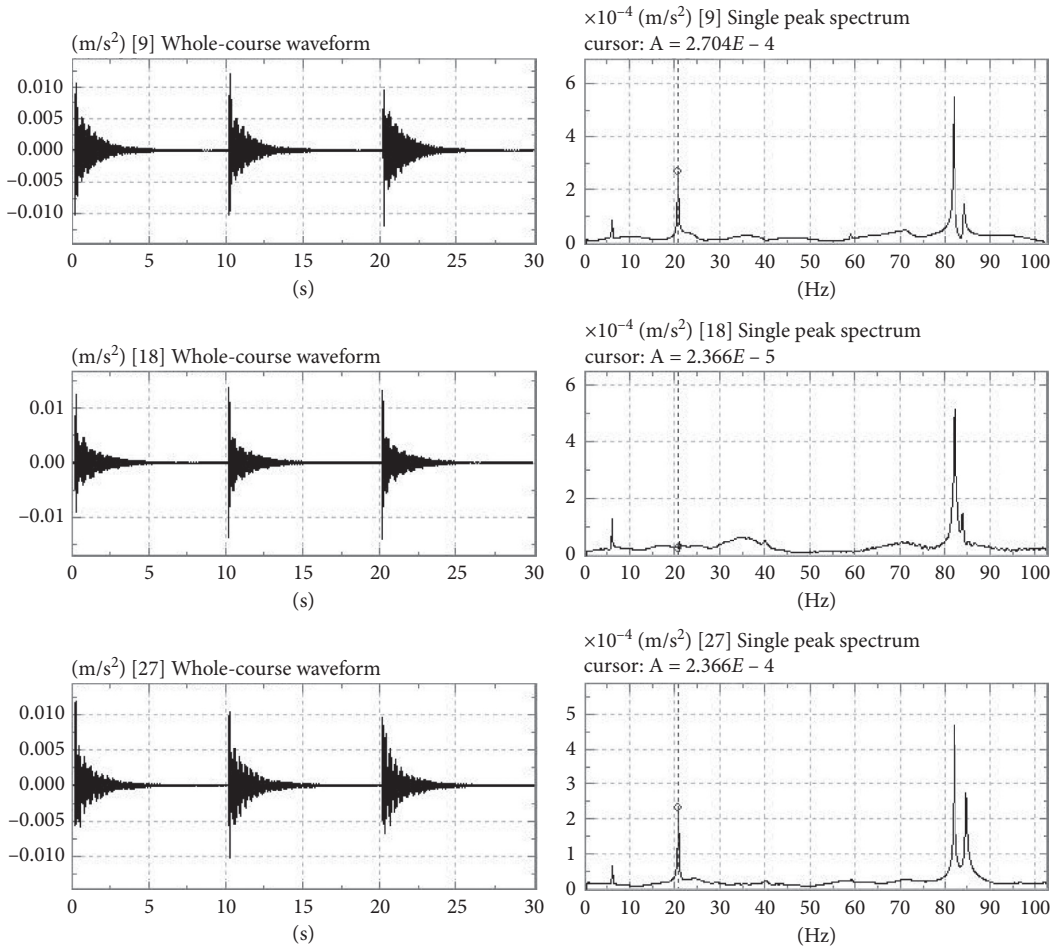

Figure 22: Spectrum curve of case 7.

structure, as shown in the following figure (take the second-order identification result as an example).

Although it is inevitable to be affected by external noise, defects of the specimens. and measurement errors in the process of testing, which may resulting in errors in the test data, the MCUIE index calculated by using the first-two modes information of the test structure can still better identify the damage of the structure. It can be seen from Figure 25 that MCUIE increases with the aggravation of damage degree, and the MCUIE values at different damage locations with the same damage degree have little difference, which can preliminarily reflect the damage degree of the structure.

The first-order damage index peak value was extracted from damage Case 7, and the relationship curve between the index peak value and the damage degree was fitted. Since the damage was two points with different damage degrees, the fitting polynomial degree was 2, and the damage degree fitting equation was as follows:

$$y = 33.14x^2 + 3.574x + 1.02, \mathrm{SSE} = 4.437e - 31. \quad (31)$$

Damage degree fitting curve of Case 7 is shown in Figure 26. Because the measured modal curvature is abnormal near the support, the MCUIE value does not start from 0. Considering the cumulative effect of structural damage, the correctness of the growth trend of the damage assessment function curve can be qualitatively verified.

6. Conclusion

Based on the sensitivity of modal curvature to damage, the information entropy index describing the degree of system uncertainty is introduced into the damage identification of beam structure. Combining with the concept of utility information entropy, the MCUIE index is proposed, and the damage identification ability of the new index and MCD is compared and analyzed by using the finite element simulation of simply supported beam.

With gapped smoothing technique adopted, the MC curve of the damaged structure is used to fit a smooth curve to replace the MC curve of the undamaged structure, which avoids the dependence on the baseline data of the undamaged structure. Through polynomial fitting of the relationship between MCUIE peak and damage degree at the damage site, the damage degree fitting equation can be obtained, which can effectively determine the damage degree qualitatively, but needs to

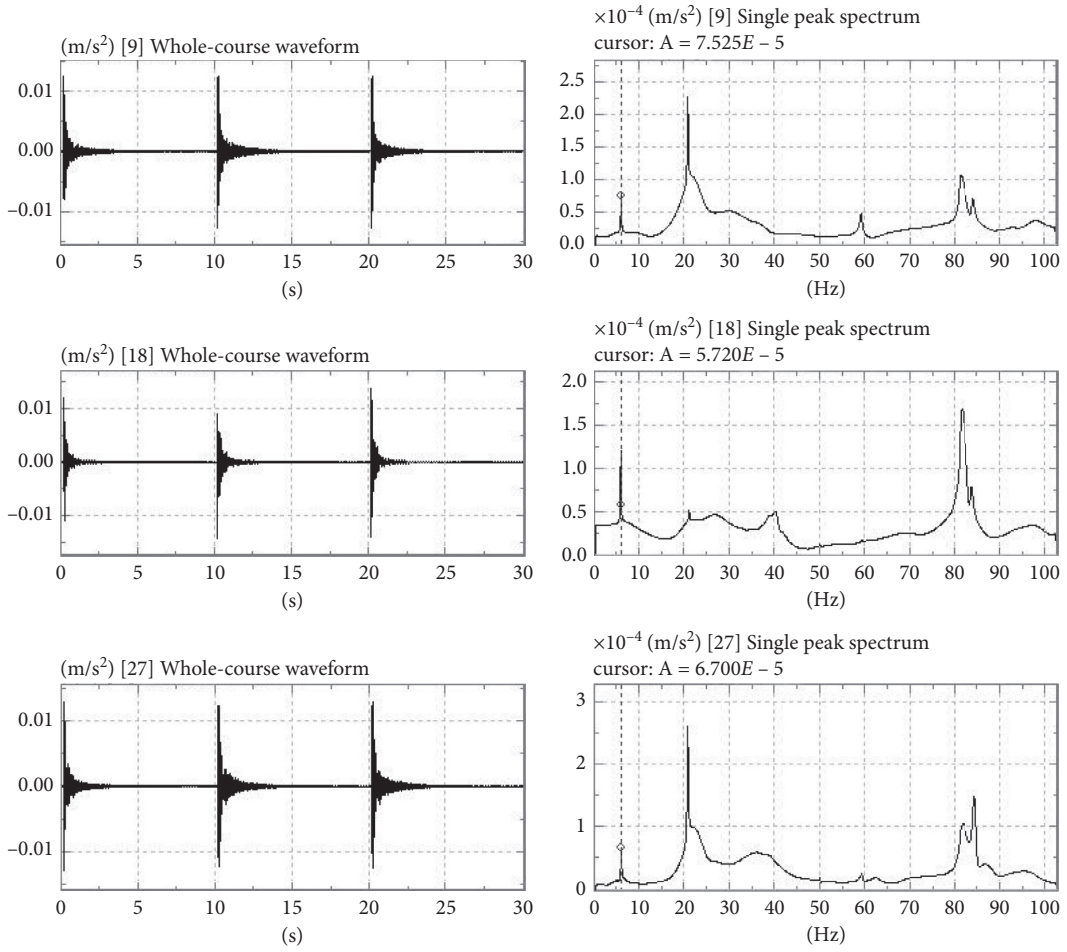

Figure 23: Spectrum curve of case 8.

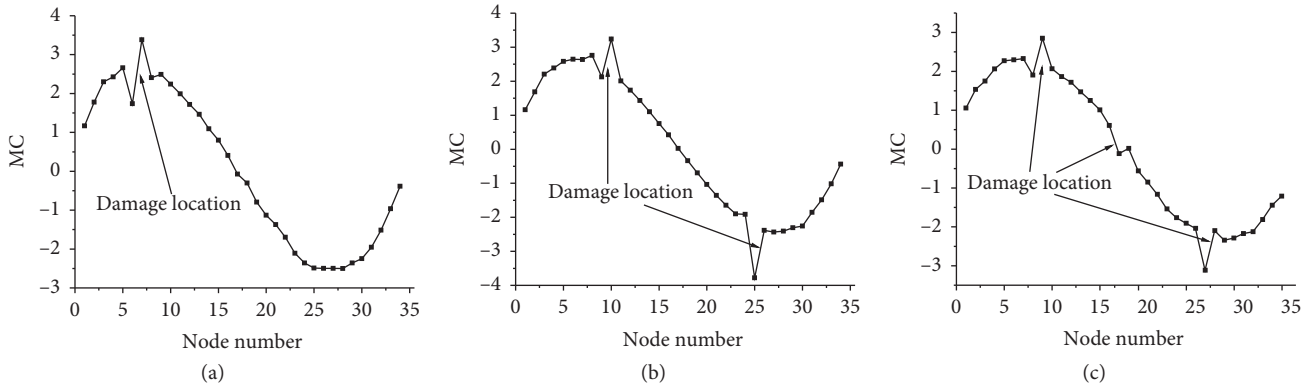

Figure 24: Damage identification result of MC. (a) Case 6. (b) Case 7. (c) Case 8.

be further optimized in the direct quantification of damage degree.

The antinoise performance of MCUIE index is analyzed by adding Gaussian white noise to the modal shapes. The results show that the index has certain noise immunity and the higher-order index has better noise immunity.

The effectiveness of MCUIE index in practical structure is verified by the damage simulation of simply supported beam model and it shows promising damage identification ability. However, due to the nonlinearity, complexity, and uncertainty of the actual structure, MCUIE index needs to be further verified in practical engineering.

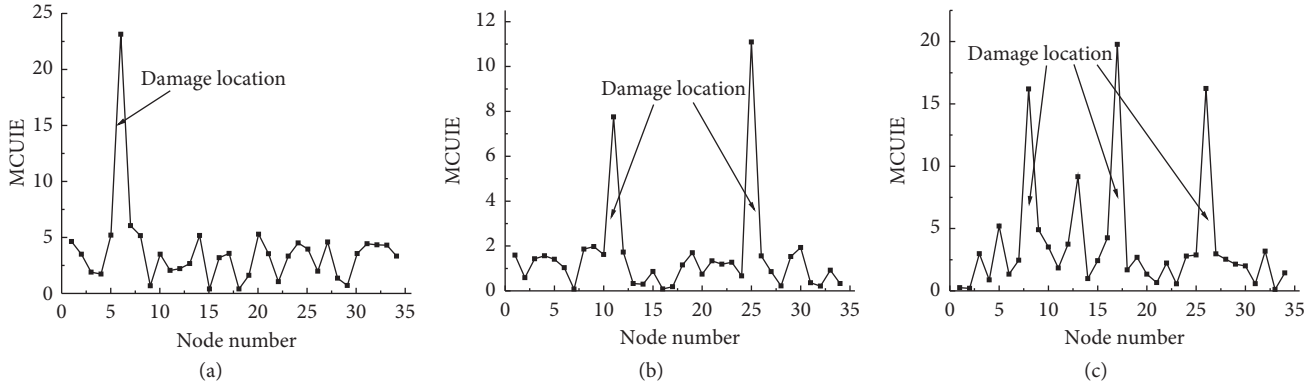

Figure 25: Damage identification result of MCUIE. (a) Case 6. (b). Case 7. (c) Case 8.

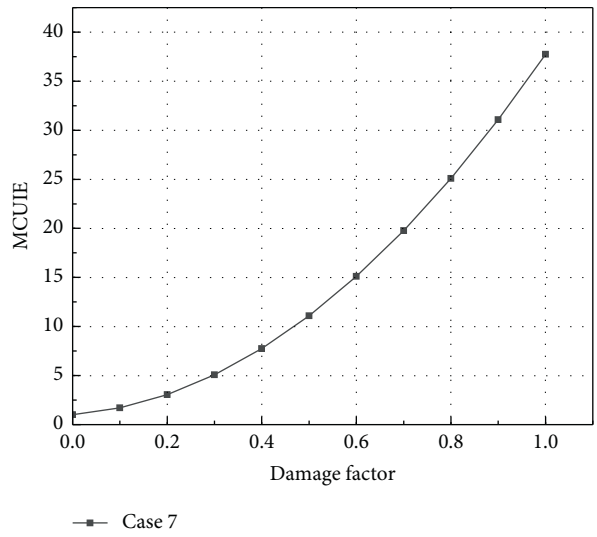

Figure 26: Damage degree fitting curve of case 7.

Data Availability

All data are available within the article or can be obtained from the corresponding author upon request.

Conflicts of Interest

The authors declare that there are no conflicts of interest regarding the publication of this paper.

Acknowledgments

This work was supported by Key Natural Science Project of Anhui Provincial Education Department (KJ2019A0746), Natural Science Foundation of China (51868045), Natural Science Foundation Youth Fund of Anhui Province (2008085QE247), and Startup Fund for Doctor of Anhui Jianzhu University (2019QDZ08).

References

[1] Y. Zhou, S. Di, C.-S. Xiang et al., "Damage identification in simply supported bridge based on rotational-angle influence lines method," *Transactions of Tianjin University*, vol. 24, no. 6, pp. 587–601, 2018.

[2] F. Han, Q.-J. Zhang, C.-F. Wang et al., "Structural health monitoring of timber using electromechanical impedance (EMI) technique," *Advances in Civil Engineering*, vol. 2020, pp. 1–9, Article ID 1906289, 2020.

[3] W. Fan and P. Qiao, "Vibration-based damage identification methods: a review and comparative study," *Structure Control Health Monitor*, vol. 10, no. 2, pp. 83–111, 2011.

[4] S. Das, P. Saha, and S. K. Patro, "Vibration-based damage detection techniques used for health monitoring of structures: a review," *Journal of Civil Structural Health Monitoring*, vol. 6, no. 3, pp. 477–507, 2016.

[5] Y. Zhou, S.-K. Di, C. Xiang et al., "Beam structure damage detection based on rotational-angle-influence-lines of elastic-constrained-support beam," *Journal of Zhejiang University (Engineering Science)*, vol. 54, no. 5, pp. 879–888, 2020.

[6] M. Bovo, M. Tondi, and M. Savoia, "Infill modelling influence on dynamic identification and model updating of reinforced concrete framed buildings," *Advances in Civil Engineering*, vol. 2020, pp. 1–16, Article ID 9384080, 2020.

[7] X. Zhou, W. Zhang, Y. Gao et al., "An experimental study of the feasibility of identifying the impact damages of reinforced

concrete piers using a modal frequency method," *Advances in Civil Engineering*, vol. 2020, pp. 1–16, Article ID 6365354, 2020.

[8] C.-Y. Kao, X.-Z. Chen, S.-L. Hung, and B. Setiawan, "Two strategies to improve the differential evolution algorithm for optimizing design of truss structures," *Advances in Civil Engineering*, vol. 2020, pp. 1–23, Article ID 4509576, 2020.

[9] W. Fan and P. Qiao, "A strain energy-based damage severity correction factor method for damage identification in plate-type structures," *Mechanical Systems and Signal Processing*, vol. 28, pp. 660–678, 2012.

[10] A. K. Pandey, M. Biswas, and M. M. Samman, "Damage detection from changes in curvature mode shapes," *Journal of Sound and Vibration*, vol. 145, no. 2, pp. 321–332, 1991.

[11] M. Cao, W. Xu, W. Ostachowicz, and Z. Su, "Damage identification for beams in noisy conditions based on teager energy operator-wavelet transform modal curvature," *Journal of Sound and Vibration*, vol. 333, no. 6, pp. 1543–1553, 2014.

[12] Z.-B. Yang, M. Radzienski, P. Kudela, and W. Ostachowicz, "Scale-wavenumber domain filtering method for curvature modal damage detection," *Composite Structures*, vol. 154, pp. 396–409, 2016.

[13] W. Xu, K. Ding, J. Liu, M. Cao, M. Radzieński, and W. Ostachowicz, "Non-uniform crack identification in plate-like structures using wavelet 2D modal curvature under noisy conditions," *Mechanical Systems and Signal Processing*, vol. 126, pp. 469–489, 2019.

[14] D. Dessi and G. Camerlengo, "Damage identification techniques via modal curvature analysis: overview and comparison," *Mechanical Systems and Signal Processing*, vol. 52-53, pp. 181–205, 2015.

[15] J. Zhang, H. Peng, and C. You, "Damage diagnosis of beam structures based on superimposed curvature modal change rate," *Engineering Mechanics*, vol. 29, no. 11, pp. 272–301, 2012.

[16] J. Ciambella and F. Vestroni, "The use of modal curvatures for damage localization in beam-type structures," *Journal of Sound and Vibration*, vol. 340, pp. 126–137, 2015.

[17] J. Ciambella, A. Pau, and F. Vestroni, "Modal curvature-based damage localization in weakly damaged continuous beams," *Mechanical Systems and Signal Processing*, vol. 121, pp. 171–182, 2019.

[18] H. Zhong and M. Yang, "Damage detection for plate-like structures using generalized curvature mode shape method," *Journal of Civil Structural Health Monitoring*, vol. 6, no. 1, pp. 141–152, 2016.

[19] M. Yang, H. Zhong, M. Telste, and S. Gajan, "Bridge damage localization through modified curvature method," *Journal of Civil Structural Health Monitoring*, vol. 6, no. 1, pp. 175–188, 2016.

[20] L. A. Overbey and M. D. Todd, "Dynamic system change detection using a modification of the transfer entropy," *Journal of Sound and Vibration*, vol. 322, no. 1-2, pp. 438–453, 2009.

[21] R. Yan and R. X. Gao, "Approximate entropy as a diagnostic tool for machine health monitoring," *Mechanical Systems and Signal Processing*, vol. 21, no. 2, pp. 824–839, 2007.

[22] C. Lohrmann, P. Luukka, M. Jablonska-Sabuka, and T. Kauranne, "A combination of fuzzy similarity measures and fuzzy entropy measures for supervised feature selection," *Expert Systems with Applications*, vol. 110, pp. 216–236, 2018.

[23] W.-X. Ren and Z.-S. Sun, "Structural damage identification by using wavelet entropy," *Engineering Structures*, vol. 30, no. 10, pp. 2840–2849, 2008.

[24] C. E. Shannon and W. Weaver, "A mathematical theory of communication," *Bell System Technical Journal*, vol. 27, no. 3, pp. 379–423, 1948.

[25] J. Zhou, C. Chen, D. J. Armaghani, and S. Ma, "Developing a hybrid model of information entropy and unascertained measurement theory for evaluation of the excavatability in rock mass," *Engineering with Computers*, vol. 5, pp. 1–24, 2020.

[26] S. F. Karimian, M. Modarres, and H. A. Bruck, "A new method for detecting fatigue crack initiation in aluminum alloy using acoustic emission waveform information entropy," *Engineering Fracture Mechanics*, vol. 223, Article ID 106771, 2020.

[27] G. Liu and Z. Wu, "New thought on dynamic identification technology for damage detection of RC structures by introducing information entropy theory," *Journal of Vibration and Shock*, vol. 30, no. 6, pp. 162–171, 2011.

[28] Z. Yang, X. Chen, Y. Jiang, and Z. He, "Generalised local entropy analysis for crack detection in beam-like structures," *Nondestructive Testing and Evaluation*, vol. 29, no. 2, pp. 133–153, 2014.

[29] R. Craig Roy, "Fundamentals of Structure Dynamics,"China Communications Press, Beijing, China, 1996.

[30] S. Naguleswaran, "Vibration of an euler-bernoulli beam on elastic end supports and with up to three step changes in cross-section," *International Journal of Mechanical Sciences*, vol. 44, no. 12, pp. 2541–2555, 2002.

[31] M. A. Koplow, A. Bhattacharyya, and B. P. Mann, "Closed form solutions for the dynamic response of euler-bernoulli beams with step changes in cross section," *Journal of Sound and Vibration*, vol. 295, no. 1-2, pp. 214–225, 2006.

[32] D. Jiang, "Information Theory and Coding,"University of Science and Technology of China Press, Hefei, China, 2008.

[33] C. P. Ratcliffe, "Damage detection using a modified Laplacian operator on mode shape data," *Journal of Sound and Vibration*, vol. 204, no. 3, pp. 505–517, 1997.

[34] Y. Jiao, H.-B. Liu, Y.-C. Cheng et al., "Damage identification of bridge based on chebyshev polynomial fitting and fuzzy logic without considering baseline model parameters," *Shock And Vibration*, vol. 2015, pp. 1–10, Article ID 187956, 2015.